



**HAL**  
open science

## Exploring charge hopping transport in amorphous HfO<sub>2</sub>: An approach combining *ab initio* methods and model Hamiltonian

Youssef Hirchaou, Benoit Sklenard, Wolfgang Goes, Philippe Blaise, François Triozon, Jing Li

### ► To cite this version:

Youssef Hirchaou, Benoit Sklenard, Wolfgang Goes, Philippe Blaise, François Triozon, et al.. Exploring charge hopping transport in amorphous HfO<sub>2</sub>: An approach combining *ab initio* methods and model Hamiltonian. Applied Physics Letters, 2024, 124, pp.052108. cea-04530721

**HAL Id: cea-04530721**

**<https://cea.hal.science/cea-04530721>**

Submitted on 3 Apr 2024

**HAL** is a multi-disciplinary open access archive for the deposit and dissemination of scientific research documents, whether they are published or not. The documents may come from teaching and research institutions in France or abroad, or from public or private research centers.

L'archive ouverte pluridisciplinaire **HAL**, est destinée au dépôt et à la diffusion de documents scientifiques de niveau recherche, publiés ou non, émanant des établissements d'enseignement et de recherche français ou étrangers, des laboratoires publics ou privés.

# Charge Hopping Transport in Amorphous Material from *ab initio* Approach

Youssef Hirchaou,<sup>1,2</sup> Benoît Sklénard,<sup>1,3</sup> Wolfgang Goes,<sup>2</sup> Philippe Blaise,<sup>2</sup> François Triozon,<sup>1</sup> and Jing Li<sup>1,3,\*</sup>

<sup>1</sup>*Université Grenoble Alpes, CEA, Leti, F-38000, Grenoble, France*

<sup>2</sup>*Silvaco-France, 38330 Montbonnot Saint-Martin, France*

<sup>3</sup>*European Theoretical Spectroscopy Facility (ETSF), F-38000 Grenoble*

Charge hopping transport is typically modeled by Marcus theory with the coupling strengths and activation energies extracted from the constrained density functional theory. However, such a method may not be a practical route for amorphous materials due to the tremendous amount of hopping paths, therefore computationally unreachable. This work presents a general approach combining the *ab initio* method and model Hamiltonian, yielding similar results to constrained density functional theory. Such an approach is computationally efficient, allowing us to consider all 23220 hopping paths between oxygen vacancies in our demonstrated amorphous hafnium dioxide model containing 324 atoms. Based on these hopping rates, charge mobility in amorphous HfO<sub>2</sub> is investigated as a function of oxygen vacancies concentration. It is found that a minimum oxygen vacancies concentration  $0.7 \times 10^{21} \text{ cm}^{-3}$  is required to enable the connectivity of the charge-hopping network.

Charge transport in amorphous materials is crucial to many technological applications, such as transistors[1–3], memories[4–6], sensors[7, 8], and batteries[9, 10]. In semi-conducting amorphous materials, the electric conduction is significantly contributed by charge hopping transport among trapping sites. Defects in oxides can serve as trapping sites, like the oxygen vacancies (OVs) in amorphous hafnium dioxide (a-HfO<sub>2</sub>) [11, 12]. The localization of a charge results in a rearrangement of surrounding atoms to minimize the system’s total energy. Therefore, a charge hopping process accompanies a collective motion of atoms, known as the reaction coordinate, since atoms are in different positions in the initial and final states. Along the reaction coordinate, the charge carrier must pass over an energy barrier, the saddle point on the energy surface connecting the initial and final states. [13] Therefore, high temperature is conducive to charge hopping, evidenced by increased conductivity with temperature [14].

Marcus theory can describe Charge-hopping transport with two essential parameters: 1) the activation energy, the minimum energy required to pass over the barrier, and 2) the coupling strength between the two trapping sites, originating from the overlap of wave functions.[13] Determining these parameters requires analyzing two energy surfaces along the reaction coordinate for the charge carrier to remain at the initial and final trap sites. The constrained density functional theory (CDFT) [15, 16] has been employed to extract these parameters for various oxide crystals[17–19]. However, the CDFT is hardly applicable to amorphous systems because of the enormous number of hopping paths, which are different. To compute all paths is computationally expensive.

In the following, we present a more computationally efficient approach by combining the *ab initio* method and model Hamiltonian to extract the required parameters in

Marcus theory. Such a method allows us to evaluate all 23220 hopping paths in our a-HfO<sub>2</sub> model. The extracted parameters are comparable to those from CDFT. Finally, we evaluated the connectivity of the hopping network and the charge carrier mobility dependence on the OV concentrations in a large a-HfO<sub>2</sub> cell.

Density functional theory with PBE functional [20] implemented in VASP [21] was used to relax atomic structure relaxation, to determine the energy of defect states, and to obtain total energy of the system either neutral or charged. A plane-wave basis set is used with a cut-off energy of 400 eV. The electronic density is converged within  $10^{-8}$  eV for the total energy. A threshold of  $10^{-5}$  eV is set for the convergence of structural relaxation. The Brillouin zone sampling is restricted at the gamma point due to the large cell of the amorphous model.

An OV in HfO<sub>2</sub> creates a defect state in the band gap. Such an OV defect state tends to trap a positive charge (hole), and the charge carrier hops in the OV network. The a-HfO<sub>2</sub> model considered here (Fig. 1(a)), which is identical to our previous work on the OV migration[12], consists of 216 oxygen and 108 hafnium atoms in a cubic cell with the edge of 16.45 Å, corresponding to the density of 8.48 g/cm<sup>3</sup> in contrast to 10.24 g/cm<sup>3</sup> in mono-clinic hafnium dioxide (m-HfO<sub>2</sub>). Fig. 1(b) shows the position of the defect state, the conduction band minima (CBM), and valence band maxima (VBM) for all possible single OV (in total 216 configurations) in the amorphous model. The position of the VBM is relatively stable, and CBM has minor variation. The defect state varies largely and spans about 2 eV. The distribution of defect state is Gaussian-like (Fig. 1(c)), similarly for double OVs of 23220 configurations (Fig. 1(d)).

The coupling strength between two OVs can be evaluated using the single-particle energy of defect states, as they directly accommodate the charge carrier. The two defect states in the case of the double OVs (A and B) are the eigenvalues ( $E_1$  and  $E_2$  shown in the insert of

---

\* Jing.Li@cea.fr

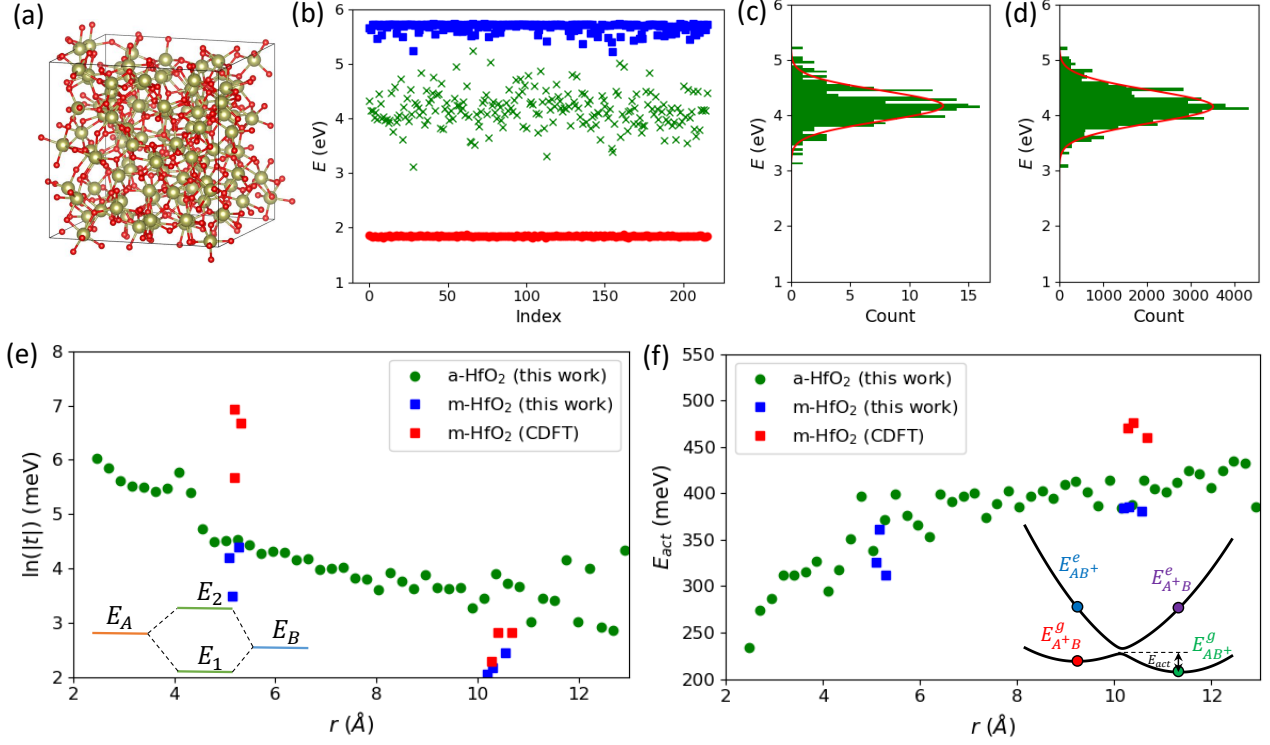


FIG. 1. Extraction of coupling strength and activation energies of charge hopping for any pair of OVs in a-HfO<sub>2</sub>. (a) The atomic structure of the a-HfO<sub>2</sub> model without any OV contains 216 oxygen and 108 hafnium atoms. (b) Defect state (green cross), valence band maxima (red dot), and conduction band minima (blue square) for single OV, which runs over all 216 oxygen sites in the a-HfO<sub>2</sub> model. The distribution of the defect states for (c) 216 single OV configurations and (d) 23220 double OV configurations. (e) The averaged coupling strength and (f) the averaged activation energy versus the distance between the two OVs. The insert in (e) demonstrates the extraction of the coupling strength from the defect state energy for structures of individual OVs ( $E_A$  and  $E_B$ ) and the structure of two OVs ( $E_1$  and  $E_2$ ). The insert in (f) demonstrates the extraction of activation energy from the four energies of the system corresponding to two ground states with the charge located at A/B OV ( $E_{A+B}^g$  and  $E_{AB+}^g$ ) and two excited states with the charge at A/B OV but atomic structure relaxed with the charge at B/A OV ( $E_{A+B}^e$  and  $E_{AB+}^e$ ). The activation energy for  $AB^+ \rightarrow A^+B$  is indicated. The coupling strength and activation energy for mono-clinic HfO<sub>2</sub> from CDFT[18] are reported in (e) and (f).

Fig. 1(e)) of the following Hamiltonian:

$$H = \begin{bmatrix} E_A & t \\ t & E_B \end{bmatrix}, \quad (1)$$

where  $E_{A(B)}$  is the energy of defect state for single OV at A(B), and  $t$  is the coupling strength. By using this method, we extracted the coupling strength of all pairs of OVs in the amorphous model. Fig. 1(e) shows the averaged coupling strength decreases with the distance between two OVs, which is as expected. In addition, we extracted the coupling strength in m-HfO<sub>2</sub>. The tendency and values are comparable to the coupling strength in a-HfO<sub>2</sub>. The values are consistent with CDFT calculation at a long distance [18]. However, some discrepancy is noticed at short-range coupling, where the CDFT yields larger coupling strength, which will be discussed later.

The activation energy for charge carrier hopping from OV A to OV B accompanies the reorganization of atomic

structures. Along the reaction coordinates  $x$ , the energy for the charge carrier stays in the OV (A or B) is a parabola under harmonic approximation, as shown by the following equations

$$E_{A+B}(x) = E_{A+B}^g + \lambda_{A+B}x^2; \quad (2)$$

$$E_{AB+}(x) = E_{AB+}^g + \lambda_{AB+}(1-x)^2; \quad x \in [0, 1], \quad (3)$$

where  $\lambda_{A+B}$  is the reorganization energy, the energy difference between the excited state  $E_{AB+}^e$  at the final coordinate and the ground state  $E_{A+B}^g$  at the initial coordinate, similarly for  $\lambda_{AB+}$ . The activation energy is evaluated at the intersection of the two energy surfaces depicted by the insert of Fig. 1(f). With the reaction coordinate at the intersection  $x_i$ , the energies are the eigenvalues of the following Hamiltonian, taking into account the tunneling,

$$H = \begin{bmatrix} E_{A+B}(x_i) & t \\ t & E_{AB+}(x_i) \end{bmatrix}. \quad (4)$$

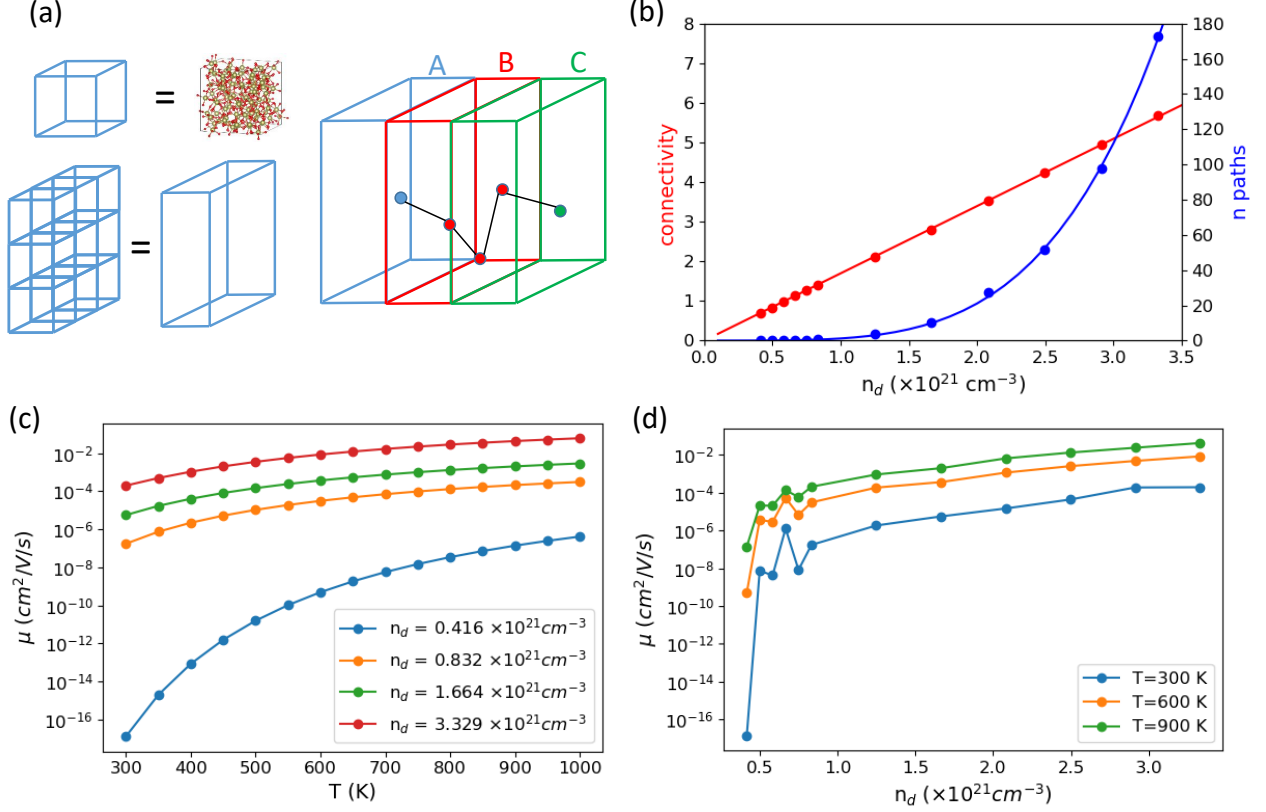


FIG. 2. Extraction carrier mobility. (a) The constructed model contains three layers: A, B, and C. Each layer is  $3 \times 3$  of the a-HfO<sub>2</sub> model. For a given OV concentration, the corresponding number of oxygen atoms is randomly removed. Mobility is evaluated by the hopping rate along the path connecting layers A and C. (b) the connectivity: the number of edges divided by the number of vertex; and the number of paths connecting A and C versus OV concentration. (c) Carrier mobility versus temperature for various OV concentrations. (d) Carrier mobility versus OV concentration at various temperatures.

The activation energy is the energy difference between the lower eigenvalue of the above Hamiltonian and the ground state energy  $E_{A+B}^g$  at the initial coordinate for charge hopping from A to B, and the difference to  $E_{AB+}^g$  for the reversed hopping direction B to A. In practice, the four energies for double vacancies can be approximately determined using single oxygen vacancy energies to avoid tremendous structural relaxation calculation:

$$E_{A+B}^g \approx E_{A+}^{A+} + E_B^B - E_0; \quad (5)$$

$$E_{A+B}^e \approx E_{A+}^{A+} + E_B^{B+} - E_0; \quad (6)$$

$$E_{AB+}^g \approx E_A^A + E_{B+}^{B+} - E_0; \quad (7)$$

$$E_{AB+}^e \approx E_A^{A+} + E_{B+}^B - E_0, \quad (8)$$

where  $E_{A+}^A$  is the energy of charged OV A (defined by the subscript) at the atomic structure with OV A relaxed at charge neutral (indicated by the superscript); similarly for other energies of single OV, and  $E_0$  is the energy free of OV. Fig. 1(f) shows the extracted activation energy in a-HfO<sub>2</sub> increases with the distance between OVs. In m-HfO<sub>2</sub>, the reorganization energy is always about 1.6 eV independent of the distance. Therefore, the ac-

tivation energy approaches  $\lambda/4 = 400$  meV at long distances and reduces at shorter distances because of the coupling strength, which shallows the energy barrier. In CDFT, the coupling strength at short range reported in Ref. [18] is larger than  $\lambda/4$ , resulting in the true ground state at the intersection between  $A^+B$  and  $AB^+$ . Therefore, the hopping transport picture depicted by the insert in Fig. 1(f) is not valid.

With the extraction of coupling strength and activation energy, we determined the hopping rate for any pairs of OVs in the amorphous model using Marcus theory [13]:

$$k_{ET} = \frac{2\pi}{\hbar} |t|^2 \sqrt{\frac{1}{4\pi\lambda k_B T}} \exp\left(-\frac{E_{act}}{k_B T}\right) \quad (9)$$

where  $k_B$  is the Boltzmann constant,  $\hbar$  the reduced Planck constant, and  $T$  the temperature.

To study the carrier mobility, we construct a larger structure consisting of 3 layers: A, B, and C. Each layer contains  $3 \times 3$  unit-cell of the a-HfO<sub>2</sub> model, as illustrated in Fig. 2(a). Considering an OV concentration  $n_d$ , the corresponding amount of oxygen atoms are removed randomly in the structure. Therefore, the structure remains

atomistic, and the hopping rates are described using parameters extracted from the *ab initio* method mentioned above. For the OV network, its connectivity is the number of edges (pairs of connected OVs) divided by the number of OVs. The carrier mobility is evaluated by the rate of transfer charges from layer A to C under an electric field  $\vec{E}$ , which shifts the parabola  $E_{AB^+}$  in Eq.3 by  $\vec{E} \cdot \vec{r}_{AB}$  given  $\vec{r}_{AB}$  the vector connects two OVs in space. Therefore, the number of paths connecting layers A and C is crucial. We studied 100 structures for each OV concentration to have a statistical sampling.

Fig. 2(b) shows the connectivity increase linearly with the OV concentration with slop of 1.7 per  $10^{21} \text{ cm}^{-3}$ , which implies that  $n_d > 0.6 \times 10^{21} \text{ cm}^{-3}$  is required for connectivity greater than unity. The number of paths connecting layers A and C increases faster at larger OV concentration and can be fitted by  $(n_d/n_0)^b$  as shown by the blue curve in Fig. 2(b), with  $n_0 = 0.96 \times 10^{21} \text{ cm}^{-3}$  and  $b = 4.12$ .

The rate of charge carrier goes from layer A to C through layer B  $k_h$  is the sum of the rate in the individual path, which is limited by the lowest hopping rate between two OVs in the path:

$$k_h = \sum_i \left( \sum_j k_{i,j}^{-1} \right)^{-1} \quad (10)$$

, where  $i$  is the index of paths connecting A and C layers, and  $j$  is the index of edges in a path. The mobility is estimated as  $\mu = k_h l_B / |\vec{E}|$ , where  $l_B$  is the length of layer B. Fig. 2(c) shows the mobility versus temperature. The temperature dependence is strong for low  $n_d$ , indicating

considerable activation energy due to the limited number of paths and large averaged distance between OVs. The mobility varies about two orders of magnitude from 300 to 900 K for larger  $n_d$ . Fig. 2(d) shows the mobility increases with OV concentrations, and the turning point is about  $0.7 \times 10^{21} \text{ cm}^{-3}$ , in agreement with the connectivity and path analysis.

By combining the *ab initio* method and model Hamiltonian, we proposed an efficient method to extract the critical parameters in Marcus theory. This method can be applied to amorphous materials to characterize tremendous hopping paths as demonstrated by a-HfO<sub>2</sub>. Also, we studied the density of the charge trapping site, which is OV in a-HfO<sub>2</sub>, and evaluated its impact on carrier mobility. It suggests a minimum OV density of  $0.7 \times 10^{21} \text{ cm}^{-2}$  is required to turn on the connectivity of the charge-hopping network.

## ACKNOWLEDGMENTS

Calculations were performed on computational resources provided by GENCI-IDRIS (Grant 2023-A0130912036 and 2024-A0150912036). This project has received funding from the European Union's Horizon 2020 research and innovation programme under grant agreement No. 871813 MUNDIFAB. For the purpose of Open Access, a CC-BY public copyright license has been applied by the authors to the present document and will be applied to all subsequent versions up to the Author Accepted Manuscript arising from this submission.

- 
- [1] S. Guha and V. Narayanan, Oxygen vacancies in high dielectric constant oxide-semiconductor films, *Physical Review Letters* **98**, 196101 (2007).
- [2] J. Robertson, High K dielectrics for future CMOS devices, *ECS Transactions* **19**, 579 (2009).
- [3] M. P. Mueller and R. A. De Souza, SIMS study of oxygen diffusion in monoclinic HfO<sub>2</sub>, *Applied Physics Letters* **112**, 051908 (2018).
- [4] F. Pan, S. Gao, C. Chen, C. Song, and F. Zeng, Recent progress in resistive random access memories: Materials, switching mechanisms, and performance, *Materials Science and Engineering R: Reports* **83**, 1–59 (2014).
- [5] A. K. Singh, S. Blonkowski, and M. Kogelschatz, Resistive switching study in HfO<sub>2</sub> based resistive memories by conductive atomic force microscopy in vacuum, *Journal of Applied Physics* **124**, 014501 (2018).
- [6] V. Antad, P. A. Shaikh, A. Biswas, S. S. Rajput, S. Deo, M. V. Shelke, S. Patil, and S. Ogale, Resistive switching in HfO<sub>2-x</sub>/La<sub>0.67</sub>Sr<sub>0.33</sub>MnO<sub>3</sub> heterostructures: An intriguing case of low H-field susceptibility of an E-field controlled active interface, *ACS Applied Materials & Interfaces* **13**, 54133–54142 (2021).
- [7] S. Ji, J. Jang, J. C. Hwang, Y. Lee, J.-H. Lee, and J.-U. Park, Amorphous oxide semiconductor transistors with air dielectrics for transparent and wearable pressure sensor arrays, *Advanced Materials Technologies* **5**, 1900928 (2020).
- [8] B. Lu, F. Zhuge, Y. Zhao, Y.-J. Zeng, L. Zhang, J. Huang, Z. Ye, and J. Lu, Amorphous oxide semiconductors: From fundamental properties to practical applications, *Current Opinion in Solid State and Materials Science* **27**, 101092 (2023).
- [9] T. Okumura, S. Taminato, Y. Miyazaki, M. Kitamura, T. Saito, T. Takeuchi, and H. Kobayashi, Lisicon-based amorphous oxide for bulk-type all-solid-state lithium-ion battery, *ACS Applied Energy Materials* **3**, 3220–3229 (2020).
- [10] S. Wu, Y. Ding, L. Hu, X. Zhang, Y. Huang, and S. Chen, Amorphous v2o5 as high performance cathode for aqueous zinc ion battery, *Materials Letters* **277**, 128268 (2020).
- [11] J. Strand, M. Kaviani, V. V. Afanas'ev, J. G. Lisoni, and A. L. Shluger, Intrinsic electron trapping in amorphous oxide, *Nanotechnology* **29**, 125703 (2018).
- [12] B. Sklénard, L. Cvitkovich, D. Waldhoer, and J. Li, Oxygen vacancy and hydrogen in amorphous hfo2, *Journal of Physics D: Applied Physics* **56**, 245301 (2023).
- [13] R. A. Marcus, Electron transfer reactions in chemistry.

- theory and experiment, *Reviews of Modern Physics* **65**, 599–610 (1993).
- [14] Z. Wang, H. Yu, X. A. Tran, Z. Fang, J. Wang, and H. Su, enTransport properties of hfo 2 x based resistive-switching memories, *Physical Review B* **85**, 195322 (2012).
- [15] B. Kaduk, T. Kowalczyk, and T. Van Voorhis, Constrained density functional theory, *Chemical Reviews* **112**, 321–370 (2012).
- [16] Q. Wu and T. Van Voorhis, Constrained density functional theory and its application in long-range electron transfer, *Journal of Chemical Theory and Computation* **2**, 765–774 (2006).
- [17] J. Blumberger and K. P. McKenna, enConstrained density functional theory applied to electron tunnelling between defects in mgo, *Physical Chemistry Chemical Physics* **15**, 2184–2196 (2013).
- [18] K. McKenna and J. Blumberger, enFirst principles modeling of electron tunneling between defects in m-hfo2, *Microelectronic Engineering* **147**, 235–238 (2015).
- [19] F. Wu and Y. Ping, enCombining landau–zener theory and kinetic monte carlo sampling for small polaron mobility of doped bivo4 from first-principles, *Journal of Materials Chemistry A* **6**, 20025–20036 (2018).
- [20] J. P. Perdew, K. Burke, and M. Ernzerhof, Generalized gradient approximation made simple, *Physical Review Letters* **77**, 3865–3868 (1996).
- [21] G. Kresse and D. Joubert, From ultrasoft pseudopotentials to the projector augmented-wave method, *Physical Review B* **59**, 1758–1775 (1999).